Available online at www.sciencedirect.com
ScienceDirect
Phytochemistry 69 (2008) 66–75
PHYTOCHEMISTRY
www.elsevier.com/locate/phytochem

Elucidation of active site residues of *Arabidopsis thaliana* flavonol synthase provides a molecular platform for engineering flavonols

Chun Song Chua [a], Daniela Biermann [a,b], Kian Sim Goo [a], Tiow-Suan Sim [a,*]

[a] *Department of Microbiology, Yong Loo Lin School of Medicine, National University of Singapore, 5 Science Drive 2, Singapore 117597, Singapore*
[b] *Department of Pharmaceutical Biology, Philipps-Universität Marburg, Deutschhausstraße 17A, 35037 Marburg, Germany*

Received 5 January 2007; received in revised form 4 June 2007; accepted 3 July 2007
Available online 24 August 2007

Abstract

Arabidopsis thaliana flavonol synthase (aFLS) catalyzes the production of quercetin, which is known to possess multiple medicinal properties. aFLS is classified as a 2-oxoglutarate dependent dioxygenase as it requires ferrous iron and 2-oxoglutarate for catalysis. In this study, the putative residues for binding ferrous iron (H221, D223 and H277), 2-oxoglutarate (R287 and S289) and dihydroquercetin (H132, F134, K202, F293 and E295) were identified via computational analyses. To verify the proposed roles of the identified residues, 15 aFLS mutants were constructed and their activities were examined via a spectroscopic assay designed in this study. Mutations at H221, D223, H277 and R287 completely abolished enzymes activities, supporting their importance in binding ferrous iron and 2-oxoglutarate. However, mutations at the proposed substrate binding residues affected the enzyme catalysis differently such that the activities of K202 and F293 mutants drastically decreased to approximately 10% of the wild-type whereas the H132F mutant exhibited approximately 20% higher activity than the wild-type. Kinetic analyses established an improved substrate binding affinity in H132F mutant (K_m: 0.027 ± 0.0028 mM) compared to wild-type (K_m: 0.059 ± 0.0063 mM). These observations support the notion that aFLS can be selectively mutated to improve the catalytic activity of the enzyme for quercetin production.

Keywords: *Arabidopsis thaliana*; Cruciferae; Flavonoids; Quercetin; 2-Oxoglutarate dependent dioxygenase; Flavonol synthase; Site-directed mutagenesis

1. Introduction

Flavonoids constitute a large group of polyphenolic secondary metabolites in plants. Approximately 8000 different flavonoid compounds have been reported to date and they have been ascribed as important for growth and normal physiology of plants (Pietta, 2000). Besides providing coloration to plants, flavonoids are important for protection against UV-B radiation and pathogenic microorganisms. The antimicrobial activities of flavonoids in plants have raised interest and further investigations have shed light on their medicinal properties (Cushnie et al., 2003; Cushnie and Lamb, 2005; Havsteen, 1983, 2002; Ormrod et al., 1995; Pietta, 2000).

The biosynthesis pathway to flavonoids has been well established and flavonol synthase (FLS) is one of the enzymes which produces quercetin **6** (Fig. 1; Harborne and Williams, 2000). This compound possesses a wide range of therapeutic properties, e.g. cardiovascular protection, anti-cancer, anti-inflammatory and anti-oxidant activities (Narayana et al., 2001). The medicinal values of quercetin **6** warrant the molecular and biochemical characterization of the enzyme responsible for its production. As a 2-oxoglutarate dependent dioxygenase (2-ODD), FLS requires 2-oxoglutarate (2-OG) and ferrous iron for catalytic function. So far, crystallographic studies of 2-ODDs have established a characteristic topology of a

* Corresponding author. Tel.: +65 65163280; fax: +65 67766872.
E-mail address: micsimts@nus.edu.sg (T.-S. Sim).

0031-9422/$ - see front matter © 2007 Elsevier Ltd. All rights reserved.
doi:10.1016/j.phytochem.2007.07.006

double-stranded beta helix (DSBH) in this protein family (Clifton et al., 2006). The DSBH consists of two sets of four beta sheets that are arranged in an anti-parallel fashion, forming a sandwich-like structure. This rigid structure provides structural support for housing two conserved motifs, Hx(D/E)x_nH and RxS, which are essential for binding ferrous iron and 2-OG, respectively. Notably, the HxDx$_n$H is the more commonly found motif in the 2-ODDs described to date (Clifton et al., 2006). This motif is known to be crucial for anchoring the ferrous iron required as a platform for dioxygen activation and subsequent catalysis (Koehntop et al., 2005; Lange and Que, 1998). While the use of a conserved mechanism involves generation of a reactive ferryl species for catalysis, studies have indicated that the 2-ODDs can carry out a variety of oxidative reactions such as hydroxylation, ring cyclization and fragmentation, epimerization and desaturation (Clifton et al., 2006). Some of these reactions are observed in four other 2-ODDs identified in the flavonoid biosynthesis pathway; flavone synthase type I (FSI), flavanone 3-hydroxylase (F3H), anthocyanidin synthase (ANS) and flavonol 6-hydroxylase (Anzellotti and Ibrahim, 2000, 2004).

FLS was first identified from a parsley cell culture by Britsch et al. (1981) and subsequently genes encoding this protein were cloned from other species such as *Petunia hybrida* (Forkmann et al., 1986), *Arabidopsis thaliana* (Pelletier et al., 1997) and *Citrus unshiu* (Moriguchi et al., 2002). Wellmann et al. (2002) reported the role of *C. unshiu* in catalyzing the desaturation of *2R,3R-trans*-dihydroflavonols **3**, **4** to flavonols **5**, **6** (Fig. 1). In the same study, the conserved ferrous iron and 2-OG binding residues were exposed by alignment with nucleotide sequences of other 2-ODDs. The two conserved residues, G68 and G261, were also identified via sequence alignment and their structural roles in the enzyme function were verified via site-directed mutagenesis (SDM). In another study, the bifunctionality of *C. unshiu* FLS was reported as it catalyzed both the conversion of *2R,3R-trans*-dihydroflavonols **3**, **4** to flavonols **5**, **6**, as well as the hydroxylation of flavanones (Lukacin et al., 2003). Interestingly, when FLS was incubated with *2S*-naringenin **1**, a natural substrate of F3H, high yields of kaempferol **5** with traces of the intermediate *2R,3R-trans*-dihydrokaempferol **3** were detected. These observations unveiled the possibility of exploiting the promiscuity of enzymes of the flavonoid biosynthesis pathway in producing novel compounds.

Hydroxylation and desaturation activities described in FLS were similarly reported for ANS, which shares

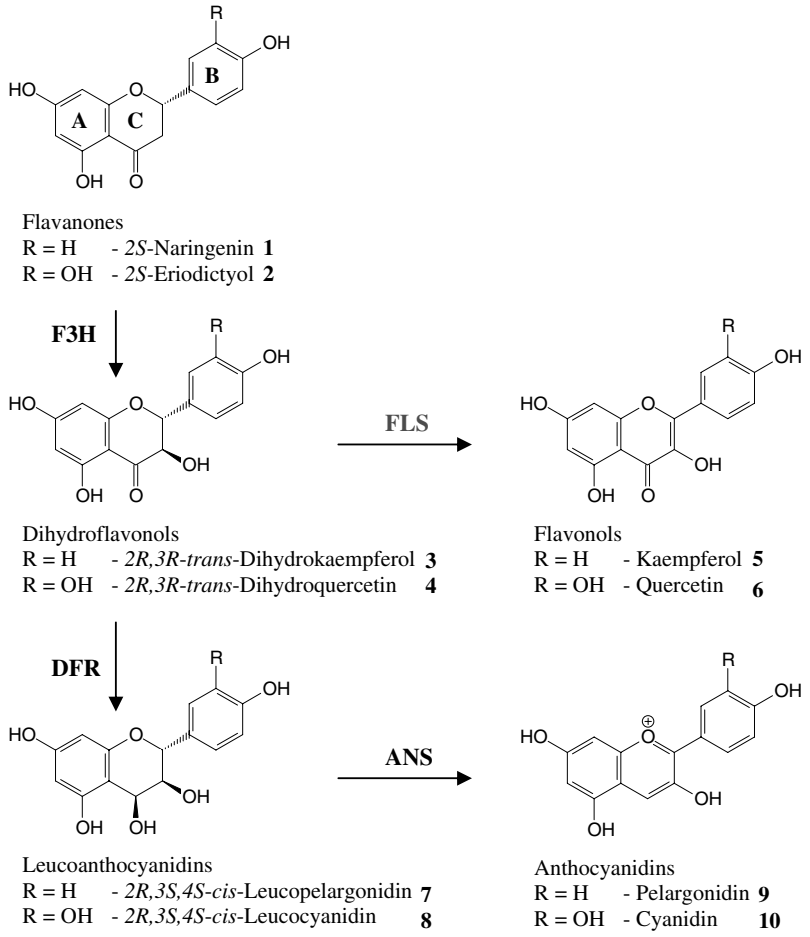

Fig. 1. Part of the flavonoid biosynthesis pathway. FLS catalyzes desaturation of dihydroflavonols to flavonols. F3H, flavanone 3-hydroxylase; FLS, flavonol synthase; DFR, dihydroflavonol reductase; ANS, anthocyanidin synthase.

approximately 50–60% sequence similarity to FLS at the polypeptide level. ANS was proposed to catalyze the *in vivo* oxidation of *2R,3S,4S-cis*-leucoanthocyanidins **7**, **8** to anthocyanidins **9**, **10**. Surprisingly, *in vitro* incubation of ANS with *2R,3S,4S-cis*-leucocyanidin **8** or *2R,3S,4R-trans*-leucocyanidin resulted in quercetin **6** being the major product formed instead of cyanidin **10** (Turnbull et al., 2003). Desaturation of *2R,3R-trans*-dihydroquercetin **4** (DHQ) to quercetin **6** in ANS was also reported (Turnbull et al., 2000), and this has supported the crystallographic study performed on *A. thaliana* ANS (aANS) where the enzyme was crystallized with *2R,3R-trans*-DHQ **4** as substrate (Wilmouth et al., 2002). Apart from the FLS-like catalytic properties, ANS was also found to be able to react with naringenin **1** (Turnbull et al., 2004). The high amino acid homology between these two enzymes, ANS and FLS, suggests a likelihood of similar three dimensional structures to support the similar catalytic reactions observed. Hence, the availability of the crystal structure of aANS with known active site residues would be useful for the characterization of other 2-ODDs in the flavonoid pathway.

In this paper, the active sites of *A. thaliana* FLS (aFLS) were first evaluated based on the crystallographic structure of aANS. Computational analyses facilitated the identification of plausible cosubstrate, cofactor and substrate binding residues in aFLS. The relevance of these residues as binding ligands was then examined by SDM and kinetic analyses of the mutants generated.

2. Results and discussion

2.1. Computational analyses

Most enzymes in the 2-ODD protein family are known to possess the HxDx$_n$H and RxS motifs for binding ferrous iron and the 2-OG, respectively. Protein sequence alignment of FLS from various species with that of aANS indicated the conserved residues in aFLS were H221, D223, H277, R287 and S289 (Fig. 2). To expose the less conserved substrate binding residues, structural modeling of aFLS was carried out. The modeled aFLS was found to be structurally similar to the crystal structure of aANS (Protein Data Bank accession number: 1GP5) (Wilmouth et al., 2002). Since the reported structure of aANS (1GP5) was complexed with DHQ **4**, which is the natural substrate of aFLS, the resolved crystal structure of aANS provided a useful platform for predicting the substrate binding residues in aFLS.

Using the Swiss-PdbViewer (SPdbV) program (Guex et al., 1999) for superimposition, the two structures were structurally aligned with a RMS value of 0.32 Å. Based on the DHQ **4** binding ligands in aANS, the residues Y142, F144, K213, F304 and E306 (Wilmouth et al., 2002) were selected and used to map out the corresponding residues in aFLS which are H132, F134, K202, F293 and E295. The latter four residues are also conserved in FLS of other species (Fig. 2), suggesting their possible structural or functional roles in the enzyme.

2.2. Choice of mutations

The functional significance of the identified residues was investigated via SDM and a total of 15 mutants were constructed. In most 2-ODDs, the ferrous iron and 2-OG are bound by the HxDx$_n$H and RxS motifs, with a few exceptions known, i.e. (1) a HxEx$_n$H motif in *Streptomyces clavuligerus* clavaminate synthase, (2) a RxT motif in *A. thaliana* gibberellin C_{20} oxidase and (3) a Kx$_n$T motif for binding 2-OG in human factor-inhibiting hypoxia-inducible factor (Elkins et al., 2003; Lukacin et al., 2000; Zhang et al., 2002). To ascertain the relevance of the putative ferrous iron and 2-OG binding residues in aFLS, they were replaced with alternative amino acids found at the corresponding positions of other 2-ODDs. The strictly conserved histidine residues were substituted with amino acids with ring structures. Hence, the mutants constructed were H221W, D223E, H277F, R287K and S289T.

Similarly, mutations were carried out on the proposed substrate binding residues. Each residue was mutated to amino acids with similar and dissimilar properties to the original residue. The dissimilar mutations constructed were, F134A, K202M, F293A, E295L and the similar mutations were F134L, K202R, F293L and E295Q. The residue H132 was mutated to a tyrosine (similar to aANS residue Y142) and phenylalanine to examine the role of any potential hydrogen bond formed between this residue and the substrate, DHQ **4**.

In addition, the secondary structures of the aFLS mutants were predicted using PSIPRED (Jones, 1999) and the results were similar to that of the wild-type (WT) (data not shown). This suggested minimal aberration in the global structure of the mutant enzymes.

2.3. Heterologous expression of soluble aFLS WT and mutant fusion proteins

The WT and mutant aFLS enzymes were expressed in *Escherichia coli* BL21 (DE3) as GST–aFLS fusion proteins. GST tag was incorporated into the enzymes for rapid purification of the fusion proteins via affinity binding to glutathione sepharose beads. Sodium dodecyl sulfate polyacrylamide gel electrophoresis (SDS–PAGE) analyses showed that the fusion proteins were solubly expressed and their levels of expression did not differ significantly from the WT. The single band which is approximately 64 kDa corresponded to the combined molecular weight of the calculated aFLS (38 kDa) and the GST protein (26 kDa) (Fig. 3). The purified fusion proteins were at least 90% pure as estimated by the Quantity One® software (Bio-Rad).

A recent study done by Welford et al. (2005) reported difficulty in determining the activities of untagged K213A

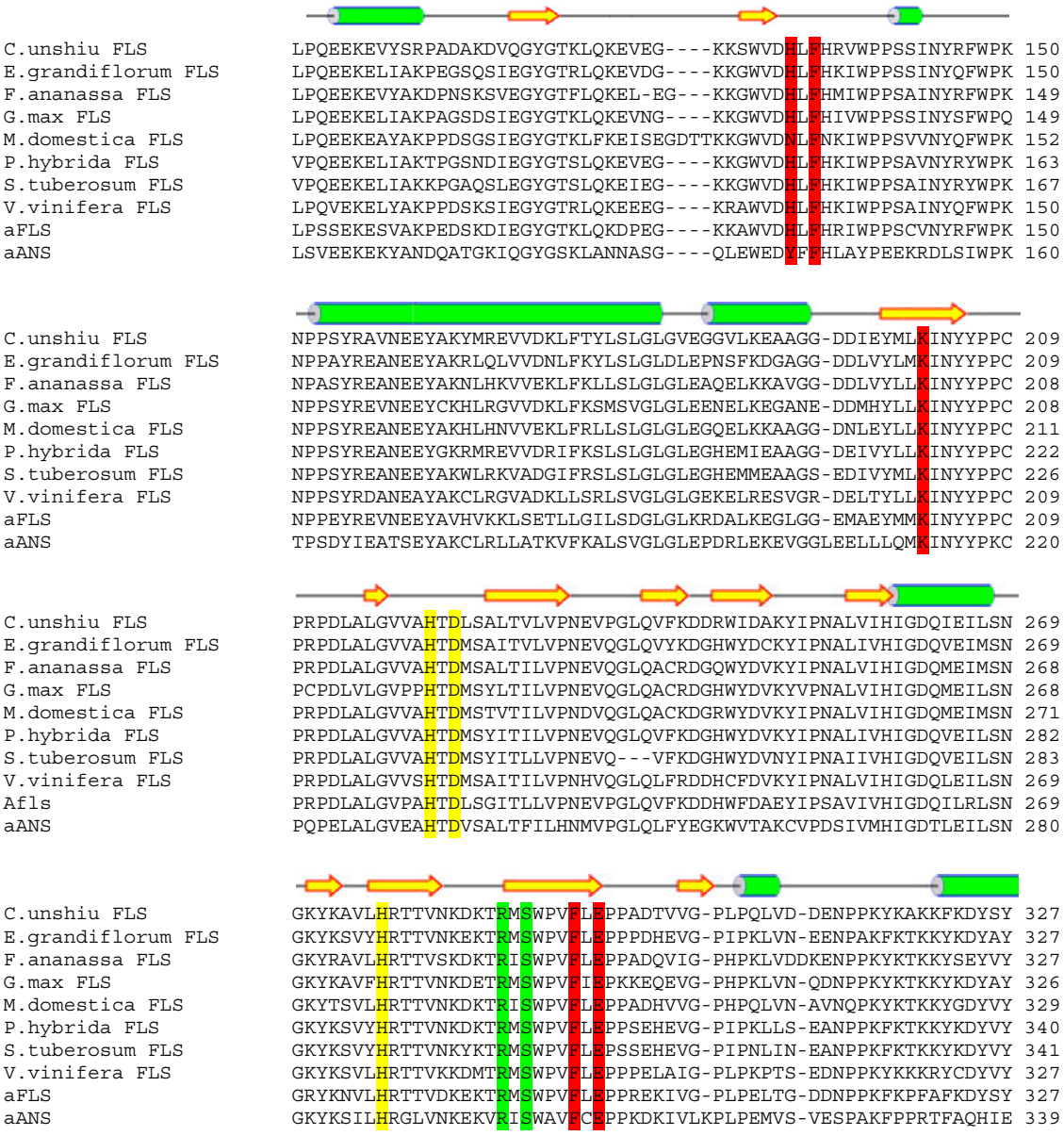

Fig. 2. Protein sequence alignment of FLS from various species with aANS. The sequence alignment indicated the amino acid residues involved in iron binding (yellow) and 2-oxoglutarate binding (green). Five potential substrate binding residues (red) were identified via superimposition of aANS and the modeled aFLS tertiary structures. The five selected residues are highly conserved in FLS of various species. The predicted secondary structure of aFLS is shown on top of the sequence alignment depicting arrangement of β-sheets (arrows) and α-helices (cylinder) in aFLS.

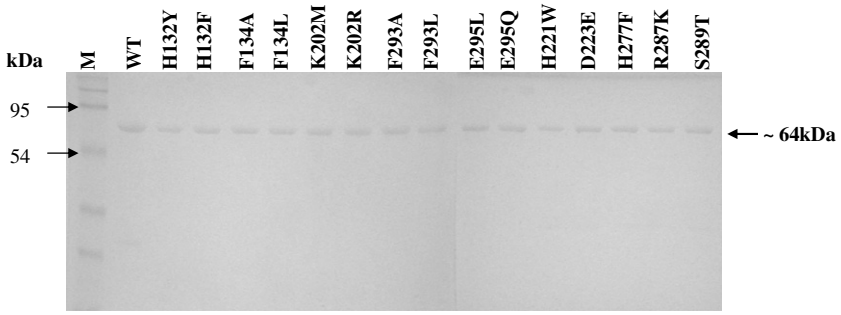

Fig. 3. SDS–PAGE analysis of WT and mutant aFLS fusion proteins obtained after purification. Lane M shows the protein standard marker (Bio-Rad) used for estimation of the protein size. All of the aFLS mutants were solubly expressed and the fusion proteins were at least 90% pure as estimated by the Quantity One® software (Bio-Rad).

(aANS) and K202A (aFLS) mutants due to insoluble protein expression. In this study, insolubility was not encountered in the expression of the mutant fusion proteins, including the K202 mutants.

2.4. Enzyme assay to determine aFLS activity

A continuous spectroscopic enzyme assay was set up in this study for efficient determination of the amount of quercetin **6** produced by the enzyme. In the previous FLS assay described by Wellmann et al. (2002), catalase was included as a component of the enzyme assay as it has been reported to provide stimulating effects for several 2-ODDs (Blanchard et al., 1982; Britsch and Grisebach, 1986; Kondo et al., 1981). However, the mechanism and function of catalase in the enzyme reaction mixture remain obscure and its use resulted in formation of a cloudy suspension. Hence, product extraction procedures were necessary prior to spectroscopic measurement. In this study, catalase was excluded without seriously compromising tangible measurements of FLS activities. Accepting a slight underrating in the activity of aFLS by omitting catalase (data not shown) enabled an easy and direct spectroscopic measurement of the product formed.

After a full spectral scan of all the components and products of the enzyme assay, a wavelength of 375 nm was found to be optimum for quantitating the amount of quercetin **6** formed in the enzyme reaction. The reagents used in the enzyme assay and succinate, the by-product formed during catalysis, had negligible absorbance reading at this particular wavelength (data not shown). The high performance liquid chromatography (HPLC) results further verified that the absorbance reading obtained at 375 nm was solely contributed by quercetin **6**, as the retention time of the converted product (single peak) coincided with that of the quercetin **6** standard (36 min) (data not shown). Hence, the spectroscopic enzyme assay was carried out in a 96-well format with the absorbance of the product measured at 375 nm. Subsequent kinetic studies of the enzymes were performed using the same assay.

2.5. Effects of mutations on the aFLS activity

To test the effects of the directed mutations on enzyme activity, the specific activities of the mutant aFLS enzymes were assayed using DHQ **4** as substrate and compared with the WT enzyme (Table 1). The specific activity of the enzyme is defined as the number of moles of quercetin produced per mg of enzyme in 1 min at 37 °C under the prescribed condition.

2.5.1. Cosubstrate and cofactor binding residues

Mutations at the proposed iron binding residues, H221W, D223E and H277F knocked out the activities of the mutants supporting the widely accepted concept that these residues are crucial for enzyme catalysis. This is also consistent with results of mutational studies performed on other 2-ODDs at similar sites (Sim and Sim, 1999; Doan et al., 2000). The abolished activity of D223E mutant clearly showed that the aspartate in the aFLS Hx**D**x$_n$H motif is non-interchangeable with a glutamate. The unique structure of clavaminate synthase that requires an amino acid with a slightly longer side-chain for securing the ferrous iron may account for the presence of a glutamate in the iron binding motif, Hx**E**x$_n$H (Zhang et al., 2002). However, in 2-ODDs with an Hx**D**x$_n$H motif, substitution to a glutamate residue would disrupt the precise arrangement of the 2-His-1-carboxylate facial triad and may render ineffective iron binding and catalysis.

Similar abolishment in the activity of R287K mutant demonstrated that this residue is crucial in aFLS. Crystallographic studies carried out on 2-ODDs showed that the conserved arginine residue would orientate the 2-OG through hydrogen bond for priming the ferrous iron (Wilmouth et al., 2002; Zhang et al., 2000). Hence, when substituted to a lysine with a shorter side, the iron priming ability of 2-OG would be reduced due to the lack of hydrogen bond support and this may lead to the loss of the enzyme activity.

On the other hand, the S289T mutant retained approximately 50% (12.9 nmol min^{-1} mg^{-1}) of WT activity (26.9 nmol min^{-1} mg^{-1}). This is similar to results of a study on F3H, where the S290T mutant retained approximately 20% of WT activity (Lukacin et al., 2000). Conversely, in *C. unshiu* FLS mutant, S289L, its activity was completely abolished (unpublished). In retrospect, these

Table 1
Specific activities and relative activities of the WT and mutant aFLSs

FLS	Specific activity (nmol min^{-1} mg^{-1})	Relative activity (%)[a]
WT	26.9 ± 5.3	100
Substrate binding sites		
H132Y	22.2 ± 4.0	83
H132F	33.4 ± 5.7	124
F134A	3.9 ± 0.4	15
F134L	14.5 ± 2.5	54
K202M	1.1 ± 0.2	4
K202R	3.3 ± 0.3	12
F293A	2.2 ± 0.2	8
F293L	2.3 ± 0.7	9
E295L	1.8 ± 0.5	7
E295Q	13.0 ± 2.5	48
Iron binding site		
H221W	ND[b]	
D223E	ND	
H277F	ND	
2-OG binding site		
R287K	ND	
S289T	12.9 ± 1.6	48

[a] Relative activity of each mutant enzyme is expressed as the percentage of the specific activity of the mutant enzyme relative to that of the WT enzyme at 100%.
[b] ND- not detectable.

results support the requirement of the serine residue in FLS and F3H for sustaining high enzyme activity.

2.5.2. Substrate binding residues

Mutations at the proposed substrate binding residues generally led to a significant decrease in the activities of the mutants except for H132F (Table 1). Most notably, the dissimilar mutations (F134A, K202M, F293A and E295L) resulted in enzymes with less than 20% of WT activity. Upon mutation to similar residues, F134L and E295Q mutants showed recovery of activities and retained approximately 50% of WT activity. However, the activities of K202R and F293L were consistently low as only 10% of WT activity was retained. The lack of recovery in the activities of K202 and F293 mutants suggest that these residues are important for substrate conversion.

Computational analyses further revealed that the residue K202 is capable of forming a hydrogen bond with the C ring of DHQ **4**. Hence, the lack of activities in K202 mutants may be attributable to the loss of hydrogen bond. Although arginine is structurally similar to lysine, the increased distance between the guanidinium group of arginine and the C ring of DHQ **4** may weaken the existing hydrogen bond. Therefore, the activities of K202R remained significantly low despite replacement with an amino acid of similar properties. On the other hand, the residue F293 was postulated to be involved in forming π stacking with the phenyl A ring of DHQ **4** as described by Wilmouth et al. (2002). As π stacking involves interaction between the electron clouds of two phenyl rings, the interaction force may be extensive. Hence, it may represent the major force responsible for binding the DHQ **4** in an optimal spatial position for desaturation to occur. The loss of the phenyl ring structures in the F293 mutants could possibly explain the diminished activities observed in the mutants.

As for the H132Y mutant, the enzyme retained approximately 83% of WT activity, whereas H132F demonstrated higher activity than WT by approximately 20%. The results clearly indicated that any hydrogen bond formed between either the tyrosine or histidine residue with DHQ **4** was non-essential. Instead, the hydrophobic environment provided by the phenylalanine side chain was preferred for desaturation of DHQ **4**. Therefore, substitution with other suitable hydrophobic amino acids can be explored for engineering aFLS with improved activities.

2.6. Kinetic analyses of WT and selected aFLS mutants

The kinetic parameters of WT, S289T, H132F, H132Y, F134L and E295Q mutants were investigated to further examine their roles in enzyme catalysis (Table 2). As for the other mutants, their specific activities were significantly lower than WT, and hence their kinetic properties were not pursued.

The K_m of H132F (0.027 mM) and H132Y (0.031 mM) mutants were approximately 2-fold lower than WT (0.059 mM). This indicates slight improvement in the substrate binding affinities of the H132 mutants and provides a basis for the improved specific activities observed in the H132F mutant. However, for the S289T and F134L mutants, their substrate binding affinities were negatively affected, as reflected by their increased K_m values. All the aFLS mutants assayed were found to exhibit an approximately 2–4-fold lower k_{cat} than WT (0.056 s^{-1}) including the H132 mutants with decreased K_m values; this implies a decreased turnover number in the mutant enzymes.

Table 2
The kinetic properties of WT and mutant aFLSs

FLS	K_m (mM)[a]	k_{cat} (s^{-1})[a]	k_{cat}/K_m (M^{-1} s^{-1})
WT	0.059 ± 0.0063	0.056 ± 0.0106	948.2
H132Y	0.031 ± 0.0040	0.030 ± 0.0022	966.5
H132F	0.027 ± 0.0028	0.034 ± 0.0037	1247.9
F134L	0.129 ± 0.0150	0.019 ± 0.0008	151.2
E295Q	0.070 ± 0.0028	0.015 ± 0.0008	208.3
S289T	0.320 ± 0.0287	0.024 ± 0.0011	75.3

[a] The results were obtained from at least three sets of independent experiments with duplicates.

2.7. Conclusion

The pronounced reduction in activities of aFLS mutants exemplified the significance of the substituted amino acid residues for enzyme catalysis and hence, further corroborated their respective recognition as ferrous iron, 2-OG, or DHQ **4** binding residues. The trends observed in the kinetic analyses of the selected mutants further supported the results of the enzyme assay and two observations were made: (1) mutations at these sites consistently led to a decrease in turnover number of the enzyme and (2) H132 is an attractive site for modification to engineer aFLS with improved activity. As these selected residues were found to be highly conserved in the FLSs of other species (Fig. 2), it is reasonable to postulate that corresponding residues in other FLSs are potentially active site residues as well. Of note, the substrate binding residues of aFLS in this study was assigned based on incubation of aFLS with DHQ **4**. Hence, further investigation is necessary to determine the roles of these residues in handling flavanones (e.g. eriodictyol and pinocembrin) as a substrate for the hydroxylation reaction.

3. Experimental

3.1. Computational analyses

Nucleotide and protein sequences of aFLS were retrieved from the GenBank Database, with accession numbers NM_120951 and NP_196481, respectively. Similarly, the FLS sequences of various species were obtained: *C. unshiu* (AB011796), *Eustoma grandiflorum* (AB078965),

Fragaria ananassa (DQ834905), *Glycine max* (AB246668), *Malus domestica* (AY965343), *P. hybrida* (Z22543), *Solanum tuberosum* (X92178) and *Vitis vinifera* (AB086055). The protein sequence of aANS (1GP5) was retrieved from the Protein Data Bank (Wilmouth et al., 2002). Subsequently, multiple sequence alignment was performed using CLUSTAL W Multiple Alignment Program (Thompson et al., 1994) to identify the conserved regions in the nucleotide sequences of FLSs in various species.

The secondary structure of FLS was predicted using the PSIPRED program (http://bioinf.cs.ucl.ac.uk/psipred/) (Jones, 1999). The tertiary structure of aFLS was predicted using SWISS-MODEL program (http://swissmodel.expasy.org/) (Schwede et al., 2003), based on comparative modeling. The "first approach mode" was selected for the modeling process and the submitted sequence (aFLS) was modeled using templates which share at least 25% sequence identity.

All protein structures were viewed using SPdbV program (http://www.expasy.org/spdbv/) (Guex et al., 1999), and this program also allowed superimposition of crystal structures. The protein structures analyzed in detail in this study were aANS (1GP5) and aFLS (predicted).

3.2. Reverse transcription of aFLS

Total RNA from the roots of *A. thaliana* was generously provided by Dr. Liu Xianan from Colorado State University. The mRNAs were purified from the total RNA through the Oligotex mRNA Mini Kit (Qiagen) in accordance with the protocol provided. After purification, the mRNAs were reverse-transcribed to obtain cDNA fragments using Sensiscript Reverse Transcriptase Kit (Qiagen). Subsequently, polymerase chain reaction (PCR) was performed to amplify the gene of interest, aFLS, using the forward (OL1231) and reverse (OL1232) primers with *Bam*HI and *Sal*I restriction sites incorporated, respectively (Table 3). The PCR protocol consisted of 1 cycle of 1 min at 95 °C followed by 35 cycles of 30 s at 95 °C, 30 s at 60 °C and 3 min at 72 °C, prior to the final extension step of 5 min at 72 °C.

3.3. Cloning of aFLS

The amplified gene products were separated via agarose gel electrophoresis using 0.8% (w/v) agarose gel. The band containing the fragment of interest, aFLS gene (~1 kb), was excised and purified using the MinElute™ Gel Extraction Kit (Qiagen) and subsequently ligated into pCR-BluntII-TOPO Vector using the Zero Blunt™ TOPO™ PCR Cloning Kit (Invitrogen). The plasmids of the positive recombinant clones were then extracted using Wizard® Plus SV Minipreps DNA Purification System from Promega. Full sequencing of both strands of the aFLS gene was carried out using the ABI PRISM™ BigDye™ Terminator Cycle Sequencing Ready Reaction Kit from Applied Biosystems to verify the recombinant vectors harboring the aFLS gene and the results were analyzed using ABI PRISM™ 3100 Genetic Analyzer.

3.4. Subcloning of aFLS

The vector containing the aFLS gene was subsequently double-digested with *Bam*HI and *Sal*I and subcloned into the expression vector, pGK (Loke and Sim, 2000). The resultant plasmid was designated as pGK-aFLS. The recombinant plasmids were transformed into *E. coli* BL21 (DE3) cells for high level expression of soluble GST–aFLS fusion protein. Similarly, sequencing was performed to identify and authenticate recombinant clones containing the gene of interest.

3.5. Heterologous expression and purification of GST–aFLS fusion protein

Recombinant cultures were grown in 50 mL Luria Bertani broth supplemented with 50 μg mL^{-1} kanamycin (Sigma) for expression studies. The cultures were grown at 37 °C with continuous agitation at 250 rpm until an OD_{600} of 0.5–0.7 was reached. They were subsequently induced with 1 mM isopropyl-β-D-thiogalactopyranoside (Sigma) and incubated at room temperature for 15 h with shaking at 250 rpm.

Following induction, the cultures were harvested by centrifugation at 7000 rpm for 5 min at 4 °C. For each preparation, the supernatant was discarded and the pelleted cells were resuspended in cold phosphate buffered saline. The cells were subsequently lysed via sonication with a 1/8″ probe at an intensity of 10 μm for 8 cycles (8 s pulse with 10 s rest in each cycle). The crude extract obtained after sonication was centrifuged at 12,000 rpm for 15 min and the soluble protein fraction (supernatant) was subsequently purified using the Microspin GST Purification Module (Amersham Pharmacia Biotech). Following the manufacturer's guidelines, each protein of interest was eluted in glutathione elution buffer (GEB). All soluble protein fractions and purified enzymes were subsequently analyzed using 10% SDS–PAGE. The images of the gel were captured using Bio-Rad Molecular Imager Gel Doc XR, equipped with the Quantity One® software. The program was also utilized to estimate the amount and purity of the expressed proteins. The purified protein concentration was measured by Bio-Rad protein assay using bovine serum albumin (Sigma) as the protein standard.

3.6. Site-directed mutagenesis

The recombinant expression vector, pGK-aFLS, was used as a template to construct aFLS mutants using QuikChange™ Site-directed Mutagenesis Kit from Stratagene (Loke and Sim, 2001). The primers required for each of the mutations were designed as shown in Table 3. Sequencing in both strands of the DNA templates was employed to

Table 3
The list of primers used in this study

Purpose	Primer	Sequence (5′–3′)
Cloning of aFLS gene into pGK vector	OL1231	*Bam*HI CCAAAA**GGATCC**ATGGAGGTCGAAAGAGTCCAAGAC
	OL1232	*Sal*I CGTATTGA**GTCGAC**TCAATCCAGAGGAAGTTTATTGAG
Mutagenesis		
Substrate binding site		
H132Y	OL1245	GGGTCGAT**TAT**CTCTTCCATCG
	OL1246	GGAAGAG**ATA**ATCGACCCAAGC
H132F	OL1270	GGGTCGAT**TTT**CTCTTCCATCG
	OL1271	GGAAGAG**AAA**ATCGACCCAAGC
F134A	OL1247	GATCATCTC**GCC**CATCGAATCTGG
	OL1248	GATTCGATG**GGC**GAGATGATCGAC
F134L	OL1272	GATCATCTC**CTC**CATCGAATCTGG
	OL1273	GATTCGATG**GAG**GAGATGATCGAC
K202M	OL1274	GCGGAGTATATGATG**ATG**ATTAACTATTATCCGCCG
	OL1275	GGCGGATAATAGTTAAT**CAT**CATCATATACTCCGCC
K202R	OL1276	GTATATGATG**AGG**ATTAACTATTATCCGCCG
	OL1277	GATAATAGTTAAT**CCT**CATCATATACTCCGC
F293A	OL1251	GGCCGGTT**GCC**TTGGAGCCTCCC
	OL1252	GGCTCCAA**GGC**AACCGGCCACG
F293L	OL1278	GGCCGGTT**CTC**TTGGAGCCTCCC
	OL1279	GGCTCCAA**GAG**AACCGGCCACG
E295L	OL1253	GGTTTTCTTG**CTG**CCTCCCCGTG
	OL1254	CGGGGAGG**CAG**CAAGAAAACCGG
E295Q	OL1280	GGTTTTCTTG**CAG**CCTCCCCGTG
	OL1281	CGGGGAGG**CTG**CAAGAAAACCGG
Iron (II) binding site		
H221W	OL1282	GTACCGGCT**TGG**ACAGATCTCAGTGG
	OL1283	CTGAGATCTGT**CCA**AGCCGGTACAC
D223E	OL1284	GCTCATACA**GAG**CTCAGTGGAATC
	OL1285	TCCACTGAG**CTC**TGTATGAGCCGG
H277F	OL1286	AATGTGTTG**TTC**AGGACGACGGTGG
	OL1287	CCGTCGTCCT**GAA**CAACACATTTTTATACC
2-OG binding site		
R287K	OL1288	GAGAAGACG**AAG**ATGTCGTGGCCG
	OL1289	CCACGACAT**CTT**CGTCTTCTCTTTATCC
S289T	OL1290	GACGAGGATG**ACG**TGGCCGGTTTTC
	OL1291	AACCGGCCA**CGT**CATCCTCGTCTTC

verify the authenticity of the desired aFLS mutants after SDM.

3.7. Assay for aFLS activity

The full spectral scan, from wavelengths 230 nm to 1000 nm (at an increment of 1 nm), was performed using the Safire, Tecan Instrument (Austria) on the components (DHQ, sodium acetate (NaOAc), sodium ascorbate (NaAsc), iron (II) sulfate, aFLS enzyme, 2-OG) and products (quercetin **6**, succinate) of the enzyme assay with controls (GEB, water) included. The optimum wavelength of 375 nm was used for measuring quercetin **6** in the enzyme assays.

Each assay reaction mixture contained 100 μM of DHQ, 111 mM NaOAc, 2.5 mM NaAsc, 42 μM iron (II) sulfate, approximately 12.5 μg of enzyme and 83 μM 2-OG (Wellmann et al., 2002). The reaction mixture was added in the order described above into a 96-well plate. Subsequently, the reaction mixture was incubated at 37 °C for 7 min prior to measuring the absorbance of the product (quercetin **6**) at 375 nm.

The same assay was carried out to determine the kinetic properties of the enzyme. Each enzyme was tested using eight different substrate concentrations (between 20 μM to 1000 μM of DHQ) and the absorbance was measured per minute for 15 min. The K_m and k_{cat} of the enzymes were determined using Hanes–Woolf plot.

Each set of experiments was performed with duplicates and the specific activities and kinetic parameters reported were based on at least three sets of independent experiments.

3.8. Verification of the product detected at 375 nm using high performance liquid chromatography

HPLC was used to verify the compound that was detected spectroscopically at 375 nm. The presence of additional compounds which could contribute to the absorbance reading at 375 nm other than the product, quercetin **6**, would be detected using the sensitive reversed-phase HPLC analysis. The liquid chromatography system used was ÄKTA purifier (Amersham Biosciences) consisting of a UV-900 detector, Autosampler A900, and a 5 μm 4.6×150 mm SunFire™ C18 column from Waters (USA). The UNICORN 5.0 program (Amersham Biosciences) was used to coordinate the operation of the chromatographic and data acquisition processes.

The enzyme assay was performed as described earlier and MeOH (70 μL) was added to stop the reaction after 7 min. The reaction mixture was centrifuged at 12,000 rpm for 5 min to pellet any precipitate. Subsequently, the supernatant was injected into the HPLC system. Solvent A (80% (v/v) of 10 mM KH_2PO_4, pH 2.0, 0.06 mM TBAB; 20% (v/v) MeOH) was used to equilibrate the column and the compound was subsequently eluted in a linear gradient of solvent A and B (100% MeOH). The elution step was carried out at 0.5 mL min^{-1} over 25 min. The absorption profiles of the compounds were monitored at 290 nm and 375 nm to detect for the presence of substrate **4** (DHQ) and product **6** (quercetin), respectively. Pure DHQ **4** and quercetin **6** (Sigma) were used as controls to verify the identity of the product formed by its retention time.

Acknowledgements

We thank Dr. Liu Xianan from Colorado State University for providing *A. thaliana* total RNA extract.

References

Anzellotti, D., Ibrahim, R.K., 2000. Novel flavonol 2-oxoglutarate dependent dioxygenase: affinity purification, characterization, and kinetic properties. Arch. Biochem. Biophys. 382, 161–172.

Anzellotti, D., Ibrahim, R.K., 2004. Molecular characterization and functional expression of flavonol 6-hydroxylase. BMC Plant Biol. 4, 20.

Blanchard, J.S., Englard, S., Kondo, A., 1982. γ-Butyrobetaine hydroxylase: a unique protective effect of catalase. Arch. Biochem. Biophys. 219, 327–334.

Britsch, L., Grisebach, H., 1986. Purification and characterization of (*2S*)-flavanone 3-hydroxylase from *Petunia hybrida*. Eur. J. Biochem. 156, 569–577.

Britsch, L., Heller, W., Grisebach, H., 1981. Conversion of flavanone to flavone, dihydroflavonol and flavonol with an enzyme system from cell cultures of parsley. Z. Naturforsch. 36, 742–750.

Clifton, I.J., McDonough, M.A., Ehrismann, D., Kershaw, N.J., Granatino, N., Schofield, C.J., 2006. Structural studies on 2-oxoglutarate oxygenases and related double-stranded β-helix fold proteins. J. Inorg. Biochem. 100, 644–669.

Cushnie, T.P.T., Lamb, A.J., 2005. Antimicrobial activity of flavonoids. Int. J. Antimicrob. Agents 26, 343–356.

Cushnie, T.P.T., Hamilton, V.E.S., Lamb, A.J., 2003. Assessment of the antibacterial activity of selected flavonoids and consideration of discrepancies between previous reports. Microbiol. Res. 158, 281–289.

Doan, L.X., Hassan, A., Lipscomb, S.J., Dhanda, A., Zhang, Z.H., Schofield, C.J., 2000. Mutagenesis studies on the iron binding ligands of clavaminic acid synthase. Biochem. Biophys. Res. Commun. 279, 240–244.

Elkins, J.M., Hewitson, K.S., McNeill, L.A., Seibel, J.F., Schlemminger, I., Pugh, C.W., Ratcliffe, P.J., Schofield, C.J., 2003. Structure of factor-inhibiting hypoxia-inducible factor (HIF) reveals mechanism of oxidative modification of HIF-1alpha. J. Biol. Chem. 278, 1802–1806.

Forkmann, G., deVlaming, P., Spribille, R., Wiering, H., Schramm, A.W., 1986. Genetic and biochemical studies on the conversion of dihydroflavonols to flavonols in flowers of *Petunia hybrida*. Z. Naturforsch. 41, 179–186.

Guex, N., Diemand, A., Peitsch, M.C., 1999. Protein modeling for all. Trends Biochem. Sci. 24, 364–367.

Harborne, J.B., Williams, C.A., 2000. Advances in flavonoid research since 1992. Phytochemistry 55, 481–504.

Havsteen, B., 1983. Flavonoids, a class of natural products of high pharmacological potency. Biochem. Pharmacol. 32, 1141–1148.

Havsteen, B.H., 2002. The biochemistry and medical significance of the flavonoids. Pharmacol. Ther. 96, 67–202.

Jones, D.T., 1999. Protein secondary structure prediction based on position-specific scoring matrices. J. Mol. Biol. 292, 195–202.

Koehntop, K.D., Emerson, J.P., Que Jr., L., 2005. The 2-His-1-carboxylate facial triad: a versatile platform for dioxygen activation by mononuclear non-heme iron (II) enzymes. J. Biol. Inorg. Chem. 10, 87–93.

Kondo, A., Blanchard, J.S., Englard, S., 1981. Purification and properties of calf liver γ-butyrobetaine hydroxylase. Arch. Biochem. Biophys. 212, 338–346.

Lange, S.J., Que Jr., L., 1998. Oxygen activating nonheme iron enzymes. Curr. Opin. Chem. Biol. 2, 159–172.

Loke, P., Sim, T.S., 2000. Mutational analysis of tyrosine191 in the catalysis of *Cephalosporium acremonium* isopenicillin N synthase. J. Biochem. 127, 585–589.

Loke, P., Sim, T.S., 2001. A comparison of three site-directed mutagenesis kits. Z. Naturforsch. 56, 810–813.

Lukacin, R., Groning, I., Pieper, U., Matern, U., 2000. Site-directed mutagenesis of the active site serine290 in flavanone 3β-hydroxylase from *Petunia hybrida*. Eur. J. Biochem. 267, 853–860.

Lukacin, R., Wellmann, F., Britsch, L., Martens, S., Matern, U., 2003. Flavonol synthase from *Citrus unshiu* is a bifunctional dioxygenase. Phytochemistry 62, 287–292.

Moriguchi, T., Kita, M., Ogawa, K., Tomono, Y., Endo, T., Omura, M., 2002. Flavonol synthase gene expression during citrus fruit development. Physiol. Plant. 114, 251–258.

Narayana, K.R., Reddy, M.S., Chaluvadi, M.R., Krishna, D.R., 2001. Bioflavonoids classification, pharmacological, biochemical effects and therapeutic potential. Indian J. Pharm. 33, 2–16.

Ormrod, D.P., Landry, L.G., Conklin, P.L., 1995. Short term UV-B radiation and ozone exposure effects on aromatic secondary metabolite accumulation and shoot growth of flavonoid-deficient *Arabidopsis* mutants. Physiol. Plant. 93, 602–610.

Pelletier, M.K., Murrell, J.R., Shirley, B.W., 1997. Characterization of flavonol synthase and leucoanthocyanidin dioxygenase genes in *Arabidopsis*: further evidence for differential regulation of early and late genes. Plant Physiol. 113, 1437–1445.

Pietta, P.G., 2000. Flavonoids as antioxidants. J. Nat. Prod. 63, 1035–1042.

Schwede, T., Kopp, J., Guex, N., Peitsch, M.C., 2003. SWISS-MODEL: an automated protein homology-modeling server. Nucleic Acids Res. 31, 3381–3385.

Sim, J., Sim, T.S., 1999. Mutational evidence supporting the involvement of tripartite residues His183, Asp185, and His243 in *Streptomyces clavuligerus* deacetoxycephalosporin C synthase for catalysis. Biosci. Biotechnol. Biochem. 64, 828–832.

Thompson, J.D., Higgins, D.G., Gibson, T.J., 1994. CLUSTAL W: improving the sensitivity of progressive multiple sequence alignment through sequence weighting, position-specific gap penalties and weight matrix choice. Nucleic Acids Res. 22, 4673–4680.

Turnbull, J.J., Sobey, W.J., Aplin, R.T., Hassan, A., Firmin, J.L., Schofield, C.J., Prescott, A.G., 2000. Are anthocyanidins the immediate products of anthocyanidin synthase? Chem. Commun., 2473–2474.

Turnbull, J.J., Nagle, M.J., Seibel, J.F., Welford, R.W.D., Grant, G., Schofield, C.J., 2003. The C-4 stereochemistry of leucocyanidin substrates for anthocyanidin synthase affects product selectivity. Bioorg. Med. Chem. Lett. 13, 3853–3857.

Turnbull, J.J., Nakajima, J., Welford, R.W.D., Yamazaki, M., Saito, K., Schofield, C.J., 2004. Mechanistic studies on three 2-oxoglutarate-dependent oxygenases of flavonoid biosynthesis. J. Biol. Chem. 279, 1206–1216.

Welford, R.W.D., Clifton, I.J., Turnbull, J.J., Wilson, S.C., Schofield, C.J., 2005. Structural and mechanistic studies on anthocyanidin synthase catalysed oxidation of flavanone substrates: the effect of C-2 stereochemistry on product selectivity and mechanism. Org. Biomol. Chem. 3, 3117–3126.

Wellmann, F., Lukacin, R., Moriguchi, T., Britsch, L., Schiltz, E., Matern, U., 2002. Functional expression and mutational analysis of flavonol synthase from *Citrus unshiu*. Eur. J. Biochem. 269, 4134–4142.

Wilmouth, R.C., Turnbull, J.J., Welford, R.W.D., Clifton, I.J., Prescott, A.G., Schofield, C.J., 2002. Structure and mechanism of anthocyanidin synthase from *Arabidopsis thaliana*. Structure 10, 93–103.

Zhang, Z.H., Ren, J.S., Stammers, D.K., Baldwin, J.E., Harlos, K., Schofield, C.J., 2000. Structural origins of the selectivity of the trifunctional oxygenase clavaminic acid synthase. Nat. Struct. Biol. 7, 127–133.

Zhang, Z.H., Ren, J.S., Harlos, K., McKinnon, C.H., Clifton, I.J., Schofield, C.J., 2002. Crystal structure of a clavaminate synthase-Fe(II)-2-oxoglutarate-substrate-NO complex: evidence for metal centered rearrangements. FEBS Lett. 517, 7–12.